Journal of Applied Electrochemistry **33**: 875–884, 2003.

Investigation of transport phenomena in a hybrid ion exchange-electrodialysis system for the removal of copper ions☆

A. MAHMOUD[1], L. MUHR[1], S. VASILUK[2], A. ALEYNIKOFF[2] and F. LAPICQUE[1,*]
[1]*Laboratoire des Sciences du Génie Chimique, CNRS–ENSIC, 47 rue Déglin, F-54042 Nancy, France*
[2]*Institute of General and Inorganic Chemistry of the National Academy of Science of Ukraine, Palladin av. 32/34, Kiev 03142, Ukraine*
*(*author for correspondence, e-mail: francois.lapicque@ensic.inpl-nancy.fr)*

Received 21 October 2002; accepted in revised form 25 February 2003

Key words: copper ions, electrodialysis, ion exchange, transport phenomena, treatment of dilute solutions

Abstract

Hybrid ion exchange electrodialysis processes allow the removal of metal ions from dilute waste liquids and the recovery of more concentrated solutions. The work reported here was aimed at investigating the two steps in the treatment process, namely, adsorption of metal ions onto the packed bed of resin and electromigration (i.e., the transport of these ions in the complex system under the applied electrical field). The case of copper sulfate was investigated. Dowex™ resins with a cross-linking degree of 2 and 8% were used. The flux of copper through the resin bed and the current efficiency for ion transfer to the cathode compartment were determined as a function of potential gradient and copper ionic fraction in the bed. Apparent diffusion coefficients of Cu^{2+} in the overall system were deduced from the experimental data.

List of symbols

A_{bed}	area of the ion exchange bed perpendicular to the potential gradient (m^2)
C	concentration (mol m^{-3})
D_{Cu}	diffusion coefficient of copper ions in the solution (m^2 s^{-1})
$D_{Cu,eff}$	apparent diffusion coefficient of copper ions in the cell (m^2 s^{-1})
$\overline{D}_{Cu}$	diffusion coefficient of copper ions in the ion exchanger (m^2 s^{-1})
ΔE_{cell}	potential difference in the cell (V)
ΔE_{empty}	potential difference in the empty cell (V)
ΔE_{bed}	potential difference in the bed (V)
F	faradaic constant (96 485 As mol^{-1})
I	cell current (A)
M	molecular weight (kg mol^{-1})
n_{Cu}	number of moles of all forms of copper recovered in cathode compartment (mol)
$n_{Cu^{2+}}$	number of moles of copper ions recovered in the cathode compartment (mol)
$n_{Cu^{2+},max}$	number of moles of copper ions recovered at infinite time (mol)
R	gas constant (J mol^{-1} K^{-1})
r_0	bead radius (m)
Re_p	particle Reynolds number
Sc	Schmidt number
T	temperature (K)
u_i	mobility of species i in the resin phase (m^2 s^{-1} V^{-1})
v	superficial velocity of the liquid (m s^{-1})
V	volume of all forms of resin in the solution (m^3)
V_H^w	volume of H-type resin in the water (m^3)
X_i	molar fraction of concentration of species i in the solution
$\overline{X}_i$	molar fraction of concentration of species i in the solid phase
z_i	valence of ion i

Greek letters

α_B^A	separation factor
δ_{bed}	thickness of the bed (m)
δ	film thickness (m)
η_{Cu}	differential current efficiency for ion i
ε	bed porosity
Φ	potential (V)
Φ_{Cu}	total current efficiency of copper transport
$\Phi_{Cu^{2+}}$	total current efficiency of copper ion transfer
τ	time constant of the process (s or h)
ξ_H	Helfferich criterion [10] (Relation 6)

☆ This paper was originally presented at the 6th European Symposium on Electrochemical Engineering, Düsseldorf, Germany, September 2002.

1. Introduction

The recovery of heavy metals from industrial process solutions has received great attention in recent years. This is mainly due to more stringent legislations for the protection of the environment. Most heavy metals are very toxic and cause great environmental damage [1, 2]. For instance, the limiting values for copper ions in Germany were reduced in the period 1983–1991 from 2 to 0.5 ppm. The conventional techniques for the removal of metal ions abatement such as hydroxide precipitation or direct electroreduction do not allow sufficient removal efficiency, and secondary treatment processes are operated downstream. An important technique for secondary treatment below ppm levels, is ion-exchange: the metal ions contained in the waste solution are exchanged by the less toxic ions contained in the fixed matrix of an ion-exchanger. Electrodialysis, an alternative technique, is an electrically driven process involving the use of ion selective membranes. This technique not only concentrates metals from the rinse streams, but also helps to maintain the quality of a plating bath. However, electrodialysis cannot be carried out at ppm concentrations. Hybrid systems combining ion-exchange with electrodialysis have been suggested to conciliate the advantages of the two individual techniques and in particular, to remove heavy metals from dilute solutions in a continuous process.

The hybrid system is obtained by inserting a bed of ion-exchanging resin into the central compartment of an electrodialysis cell. This compartment is located between two ion-selective membranes that essentially divide the cell into three separate compartments. Water electrolysis occurs in the two external electrode compartments, and H^+ formed at the anode is to transferred to the resin bed.

Combination of electrodialysis and ion-exchange for removal of ions from solution has received great attention. One of the first to mention such a combination was Glueckauf [3] for the treatment of radioactive wastes, Much of the work, however, has focused on the production of ultrapure water, as claimed in the Millipore process [4, 5]. This method was first presented at the Achema Fair in Frankfurt, Germany, in 1994, and has been developed at the Research Centre Jülich [6] for the prediction of ion exchange and electrochemical regeneration of ion exchangers in ultrapure water production. The above process was used for the removal of monovalent metals. These ions have a much greater mobility in the exchanger when compared to divalent metals such as copper [7] and can thus be removed with much greater ease. The combined technique was investigated for the case of Ni^{2+} ions [8, 9], and the migration rate of the ions in the resin bed was shown to depend strongly on the resin flexibility and on the intensity of the electrical field, as expected.

The present paper deals with investigations of the technique for Cu^{2+} removal from a copper sulfate solution using a three-compartment cell similar to that used for the case of Ni^{2+} [8, 9]. The two elementary processes, namely the adsorption of the metal ion and the migration in the resin bed and through the membrane have been investigated separately. Two ion-exchange materials with different flexibility levels were used. First, the equilibrium between an ion exchanger and a solution of copper sulfate in sulfuric acid was carefully determined. Then, the migration rate of Cu^{2+} was measured depending on the potential gradient across the bed and the concentration of Cu^{2+} ions.

2. Sorption isotherm of the Cu^{2+}/H^+ system

The active sites of the resin are occupied by H^+ ions in competition with Cu^{2+} species, depending on various parameters, and mainly the solution pH. The equilibrium between an ion exchanger and a solution of copper sulfate in sulfuric acid was carefully studied to predict the capacity of the ion exchangers and their selectivity coefficient.

2.1. *Theory [10–13]*

The monodivalent ion exchange process between Cu^{2+} and H^+ is represented by Equation 1:

$$2H^+_{resin} + Cu^{2+}_{solution} \rightleftharpoons Cu^{2+}_{resin} + 2H^+_{solution} \tag{1}$$

The selectivity coefficient of the ion-exchange process can be defined on the basis of concentrations or mole fractions. On the latter basis, $K_{X,Cu/H}$ is expressed as

$$K_{X,Cu/H} = \left(\frac{\overline{X}_{Cu^{2+}}}{X_{Cu^{2+}}}\right) \times \left(\frac{X_{H^+}}{\overline{X}_{H^+}}\right)^2 \tag{2}$$

where X_i and $\overline{X}_i$ are the equivalent ionic fractions of species i in the solution and in the resin phase, respectively. The equivalent fractions of Cu^{2+} and H^+ are defined as

$$X_{H^+} = \frac{[H^+]}{2[Cu^{2+}] + [H^+]} \qquad X_{Cu^{2+}} = \frac{2[Cu^{2+}]}{2[Cu^{2+}] + [H^+]} \tag{3}$$

$$\overline{X}_{H^+} = \frac{[\overline{H^+}]}{2[\overline{Cu^{2+}}] + [\overline{H^+}]} \qquad \overline{X}_{Cu^{2+}} = \frac{2[\overline{Cu^{2+}}]}{2[\overline{Cu^{2+}}] + [\overline{H^+}]} \tag{4}$$

where $[\overline{Cu^{2+}}]$ and $[\overline{H^+}]$ are the ion concentrations in the ion-exchanger phase, and $[Cu^{2+}]$ and $[H^+]$ are the concentrations of ions in the solution. The phase equilibrium can also be described by the separation factor, α^{Cu}_H, defined as

$$\alpha^{Cu}_H = \left(\frac{Y_{Cu^{2+}}}{\overline{X}_{Cu^{2+}}}\right) \times \left(\frac{\overline{X}_{H^+}}{Y_{H^+}}\right) \tag{5}$$

The essential difference between the separation factor and the selectivity coefficient is that the latter contains the ionic valences as exponents. The total normality of the solution is defined as the sum $[H^+] + 2[Cu^{2+}]$.

2.2. *Experimental details*

Two styrene-based cation exchangers Dowex™ were used:

(i) A cation exchanger Dowex HCR-S, with 8% degree of cross-linking (Divinylbenzene, DVB) and a size distribution of 20–50 mesh, that is, from 297 to 841 μm.

(ii) A less stiff resin, Dowex 50WX-2 in the H^+ form, where the degree of cross-linking (DVB) is only 2%. Its size distribution is 50–100 mesh, that is, from 150 to 297 μm.

The experiments were carried out at room temperature with mixed $CuSO_4$ and H_2SO_4 solutions of various concentrations by fixing the total normality at 0.5 (equiv.) l^{-1}. The composition of these solutions was calculated using a thermodynamic model of the mixed solution for various proportions of copper salt over sulphuric acid, with the total normality at 0.5 (equiv.) l^{-1}. The model derived from previous investigations of the $ZnSO_4$–H_2SO_4 system [14] takes into account the nonideal behaviour of the various species by means of the Pitzer model for the various interactions. In addition, the partial dissociation of copper sulfate was also accounted for, as recommended in [15]. Figure 1 shows the results of the model, in terms of the variation of the amount of copper sulfate to be introduced, pH of the mixed solution and $X_{Cu^{2+}}$, with the concentration of sulfuric acid introduced. As expected, the dissociation of copper sulfate is not complete and from 20 to 35% of the copper sulfate introduced remains in the form of ion-pairs. Contrary to most investigations dealing with ion-exchange, the sorption equilibrium of Cu^{2+}/H^+ was determined considering the actual concentrations of ions, and not the concentrations of the electrolytes introduced for the preparation of the solution.

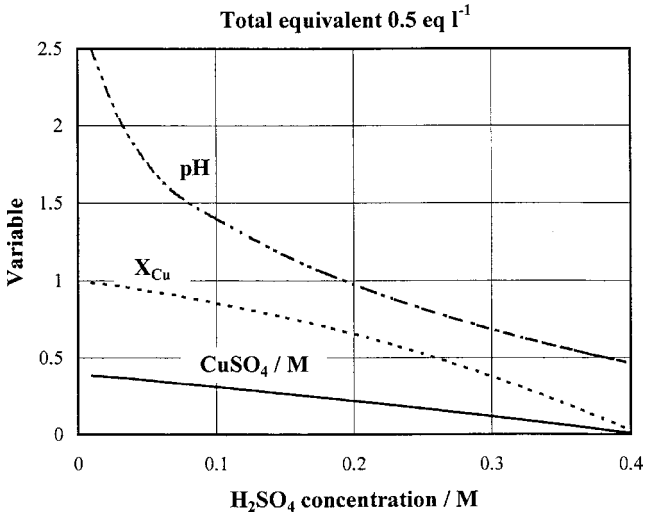

Fig. 1. Thermodynamic equilibrium of a mixed $CuSO_4$–H_2SO_4 solution at 25 °C with total normality of 0.5 (equiv.) l^{-1}: pH, mole fraction of copper ion in the solution and concentration of copper sulfate to be introduced in preparing the solution.

The sorption equilibrium was determined by continuous percolation of a large volume of the mixed solution considered through the resin bed. Two beds were used: (i) a small glass column, 6.5 cm long and 1 cm in diameter, and (ii) the central compartment of the electrodialysis cell, described in the following Section, being 10 cm high and with a cross section of 1.5 cm^2.

The solution was driven into the resin bed by a peristaltic pump at 2 cm^3 min^{-1} for the 1 cm column, and 5 cm^3 min^{-1} in the central compartment of the cell. Preliminary measurements showed that a volume of liquid over fivefold the volume of the bed allowed the equilibrium to be attained, corresponding to identical compositions of the inlet and outlet solutions.

When the resin and the solution were in equilibrium, the bed was quickly rinsed with deionised water to remove the electrolyte contained in the liquid between the resin particles. The resin bed was then regenerated by injection of 2 M H_2SO_4 and the quantity of Cu^{2+} was determined by titration of the recovered acid solution with EDTA.

2.3. *Results and discussion*

The capacity of the two ion-exchange resins was first determined using a 0.385 M copper sulfate solution corresponding to a total normality of 0.5 (equiv.) l^{-1} and $X_{Cu^{2+}} = 1$. The capacity of the 50WX-2 and HCR-S grades was found at 0.76 and 1.80 (equiv.) l^{-1}, respectively: replicate experiments yielded these values with an accuracy of 2%. The concentration of H^+ in the resin was deduced from the concentration of Cu^{2+} taking into account the valence of the latter ion, and led to the equivalent ionic fraction of Cu^{2+} in the resin, $\overline{X}_{Cu^{2+}}$. The values of the equivalent ionic fractions $X_{Cu^{2+}}$ and $\overline{X}_{Cu^{2+}}$ allowed the selectivity coefficient and the separation factor to be calculated for each solution. The average values of the two variables were deduced and used for fitting of the experimental data, as shown in Figure 2.

The results obtained with the two beds of HCR-S resin are perfectly similar (Figure 2). The isotherm profile indicates that copper is strongly preferred by this resin over protons. A similar comment can be made for the less rigid resin even though the affinity of the resin for Cu^{2+} ions is slightly weaker. For both resins, the simple laws for the sorption isotherm fit well with the experimental data.

The preference of ion exchangers for one ion over another is often expressed by the separation factor. It is well known that in the case of divalent–monovalent exchange, the separation factor is a decreasing function of the total ion concentration in the bulk solution [10]. The values of the average selectivity coefficient were found to be 9.5 and 13.7 for the 2% and 8% cross

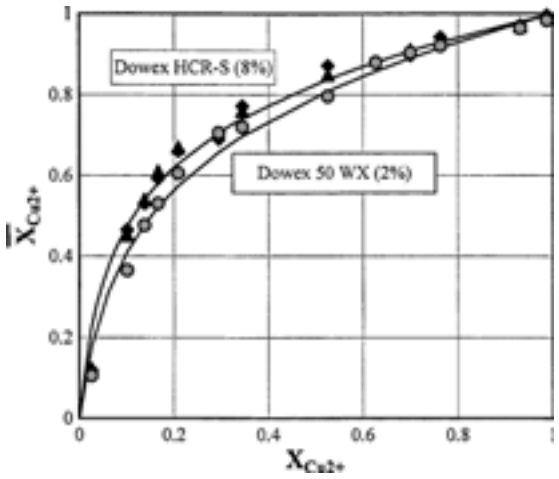

Fig. 2. Sorption equilibrium of copper ion on two resins investigated. Solid lines correspond to fitting after Relation 2 and average value of the selectivity coefficient.

Table 1. Selectivity coefficient and separation factor of the two Dowex resins used with a 0.5 (equiv.) l^{-1} total concentration in solution

Resin	Selectivity coefficient $K_{X,Cu/H}$	Separation factor α_H^{Cu}
50 WX-2 (2%)	9.5 ± 2.8	4.2 ± 1.7
HCR-S (8%)	13.7 ± 3.9	6.1 ± 1.7

linking resins respectively, in fair agreement with the literature [16, 17]. For the exchange of inorganic ions [17], the selectivity coefficient increases with the DVB degree, because the affinity of resins for an ion is governed by the dimension of the hydrated ion, and therefore by the change in its structure to accommodate the ion. Accordingly, a higher separation factor is allowed for the more rigid resin (Table 1).

3. Transport phenomena in the process investigated

3.1. *Diffusion of ions in the resin beds*

As ion exchange is in most cases a diffusion process, the rate-controlling step is the interdiffusion of counter ions to and from ion exchanger particles. Two rate-controlling steps frequently considered are particle diffusion control and film diffusion control: both of them are governed by the resin properties and the operating conditions. A relatively simple criterion based on a dimensionless modulus was suggested by Helfferich [10] to predict the nature of the rate-controlling step:

$$\xi_H = \frac{(5 + 2\alpha_H^{Cu})}{r_0} \times \delta \frac{[\overline{Cu^{2+}}]}{[Cu^{2+}]} \times \frac{\overline{D}_{Cu}}{D_{Cu}} \qquad (6)$$

where δ is the thickness of the diffusion layer at the external surface of the resins particles with a radius r_0, and $\overline{D}_{Cu}$, the diffusion coefficient of Cu^{2+} in the resin

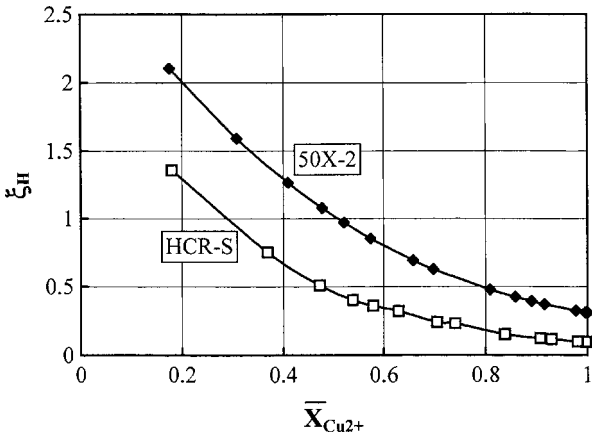

Fig. 3. Calculated variation of the ξ_H for internal/external diffusion with bed of resins, with molar fraction of copper ion in the resin.

structure. This criterion is homogeneous to the ratio of the external transfer rate to the internal diffusion rate. Values of ξ_H far below unity correspond to particle diffusion control whereas the control from the external mass transfer prevails for ξ_H far above unity.

Two parameters, δ and $\overline{D}_{Cu}$, required for estimation of the diffusion criterion were estimated, and details in the calculated procedure are given in the Appendix. Values for $\overline{D}_{Cu}$ were estimated at 8.7×10^{-11} and 1.13×10^{-11} m^2 s^{-1} for the 50WX-2 and HCR-S resins, respectively. Concentrations in the resin and in the solution were calculated at equilibrium from the sorption isotherm, depending on $\overline{X}_{Cu^{2+}}$. As shown in Figure 3, ξ_H is a decreasing function of $\overline{X}_{Cu^{2+}}$, due to the nonlinear profile of the sorption isotherm. For the more rigid resin, ξ_H varies from 1.3 to 0.2, indicating slow diffusion in the resin particles, even though the external diffusion exerts a noticeable control of the transfer phenomena. Internal diffusion seems to be faster in the 50WX-2 grade (Figure 3), corresponding to mixed control by the two diffusion processes.

3.2. *Ion transport in the presence of an electrical field*

In the presence of an electrical field, charged species are mainly transported in the bed by convection, diffusion and migration. Even though the occurrence of convection phenomena in the resin bed has been reported in a few papers, there is no means to quantify its significance and convection is neglected in most cases. For sufficient intensity of the electrical field, diffusion fluxes are much smaller that the flux generated by migration. As assumed previously by Spoor et al. [8] it can then be assumed that the Nernst–Planck equation applied to the resin bed in the presence of an electrical field reduces to the migration term:

$$\vec{N}_{Cu} = -z_{Cu} C_{Cu^{2+}} u_{Cu} \overrightarrow{\text{grad}}\ \Phi \qquad (7)$$

where the mobility of Cu^{2+} is linked to the apparent diffusion coefficient:

$$u_{Cu} = \frac{D_{Cu,eff}F}{RT} \quad (8)$$

The transport of charges in the resin can occur (i) through the resin particles, or (ii) in the liquid film surrounding the solid particles. The concentration appearing in Equation 7 refers to the solid resin or to the solution, depending on the transport process. Process (i) predominates when the conductivity of the liquid is very low, as for the present case when deionized water is injected (Section 4.1). Conversely, process (ii) could be the more significant in case that the conductivity in the liquid largely exceeds that of the resin, as for concentrated solutions. For the present case of a resin bed inserted between two ion membranes, two additional processes have to be considered: (iii) the internal transport through the membrane solution, and (iv) the external transport in the stagnant film at the membrane surface.

Thorough investigation of transport phenomena in the process of interest is of high complexity. Therefore, as explained in Section 4, transport phenomena were observed through the overall flux of copper ions accumulated in the cathode site. This flux results from desorption from the resin particles, transport through the bed, and transfer through the membrane. The measurement of the overall flux led to apparent diffusivity $D_{Cu,eff}$.

4. Electromigration of copper ions in ion-exchanger resins

4.1. *Experimental details*

The experimental cell was a three-compartment device (Figure 4) 10 cm high and machined out of Perspex material. The resin bed was prepared in the central compartment 15 mm wide and 10 mm deep. The 5 mm compartments near the electrodes, were separated from the resin bed by cationic membranes (Nafion™ 117). Both electrodes were platinum-coated titanium plates. The bed was continuously percolated downward by the considered solution at flow rates up to 10 cm^3 min^{-1} using a peristaltic pump (BVK, Ismatec). A sulfuric acid solution at 0.5 M was continuously circulated in each electrolytic compartment at 30 l h^{-1} by a centrifugal pump (Iwaki) through a flow meter and a tank reservoir.

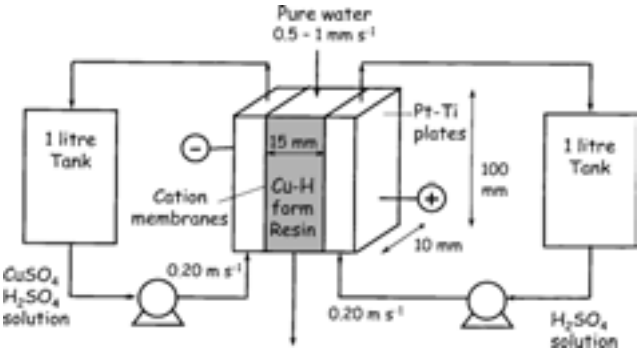

Fig. 4. Schematic view of experimental set-up for electromigration experiments.

The experiments were performed at room temperature, around 22 °C. Prior to electromigration experiments, the resin bed was loaded with copper ions upon continuous percolation of the selected ($CuSO_4$–H_2SO_4) solution with a total normality of 0.5 (equiv.) l^{-1}, at 5 ml min^{-1}. The impregnation was stopped for a volume of percolated solution tenfold the volume of the bed (15 cm^3). The bed was rapidly rinsed with 2 volumes of deionized water. Then deionized water was passed once at 5 ml min^{-1} through the ion-exchange bed while a constant voltage was applied between the electrodes. The current was continuously measured using a calibrated 1 ohm resistor inserted in the circuit. The pH of the liquids was measured at the outlet of the three compartments of the cell. Samples of the three liquids were taken on a 15 min basis for 4 h experiments and every 30 min for longer-term runs. The fractions with a copper concentration below 100 ppm were analysed by air–acetylene 'flame atomic absorption', in particular for determination of the mole number of copper ion in the cathode side. After switching off the electrical supply, the bed was percolated with a 2 M sulfuric acid solution for desorption of the remaining copper ions. The cell was taken apart and the cathode was immersed in dilute nitric acid for dissolution of the traces of metal formed by side-electroreduction of copper ions. Both liquid fractions were submitted to chemical analysis.

The resin bed was loaded with various amounts of copper for investigation of the electromigration: $\overline{X}_{Cu^{2+}} = 0.98$, 0.61 and 0.36 for Dowex 50 WX-2, and $\overline{X}_{Cu^{2+}} = 1.00$, 0.73 and 0.47 for Dowex HCR-S.

4.2. *Experimental observations*

During experiments, a front of ion-exchange was observed to form and to move towards the cathode where both H^+ and Cu^{2+} ions migrate with different rates because of their different mobility [10]. As a rule, a zone of dark blue colour is visible at the top of the bed after one hour. This zone corresponds to a Cu^{2+} concentration in the solution higher than the value predicted by sorption equilibrium. The phenomenon evidenced by visual observations may be due to the accumulation of copper ions in the region induced by the rate-controlling transfer of Cu^{2+} ions through the membrane. On the other hand, the orange zone corresponding to H^+-form resin extended towards the cathode. Figure 5 shows the aspect of the bed of Dowex 50 WX-2 after one hour and at the end of the experiment. At this time, the front is fairly visible in the bed and H^+-form resin predominates in the lower part of the bed and closer to the anode membrane. For the HCR-S resin initially saturated with copper ions, two main zones are observed as for the 50WX-2 resin, but the front of ion exchange is less clearly defined, with a progressive change in composition of the resin between

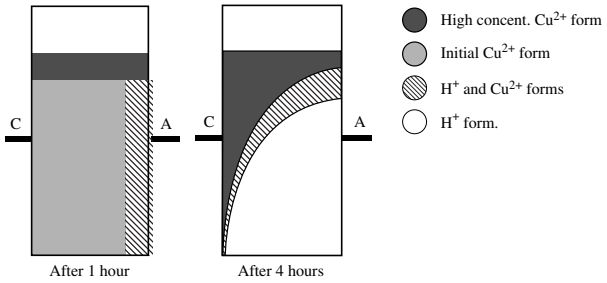

Fig. 5. Schematic view of resin bed (Dowex 50 WX-2) during electromigration experiments. A and C refer to electrode polarity.

the two zones. When the bed of HCR-S resin is not fully loaded at the closure of the electrical circuit, the front of ion exchange and the predominant zones cannot be defined accurately in the bed whose composition is to be more uniform. The local change in aspect of the bed presented above, corresponds to local changes in the bed conductivity and the current distribution is probably far from uniform, in particular with the 50 WX-2 resin.

The pH of the three solutions sampled, changed very little during the batch experiments. In particular, the pH of the sulfuric acid solutions remained near 0.6, with a slight increase at the cathode side due to production of OH^- ions. The solution leaving the central compartment has a pH near 3.3 within 0.3, due to the flux of H^+ transferred from the anode side. The copper contents of the various liquids are given and discussed in Section 4.4.

4.3. *Potential gradient and current in the cell*

The average potential gradient in the bed was calculated considering a one-dimensional model, that is, assuming that the current lines are perpendicular to the electrode planes. The average gradient was then expressed as the ratio of the ohmic drop in the bed, ΔE_{bed}, over its thickness, δ_{bed}:

$$\nabla\Phi = \frac{\Delta E_{bed}}{\delta_{bed}} \tag{9}$$

The ohmic drop in the bed was deduced from the total cell voltage, ΔE_{cell}, by subtracting the potential differences in the two electrode compartments and the membrane. For estimation of these two contributions, the fixed bed was replaced by a 0.5 M H_2SO_4 solution and the voltage in the resin-free cell, ΔE_{empty}, was measured depending on the applied current I. The ohmic drop in the central liquid vein, $RI_{central}$, was estimated from the conductivity of the electrolyte solution at 22 °C (0.21 Ω^{-1} cm^{-1}) and the channel dimensions. This contribution had to be subtracted from the voltage in the empty cell, ΔE_{empty}. ΔE_{bed} was therefore calculated as

$$\Delta E_{bed} = \Delta E_{cell} - (\Delta E_{empty} - RI_{central}) \tag{10}$$

The cell voltage was fixed below the empirical threshold corresponding to a maximal current of 250 mA. As a matter of fact, too high currents with uneven distributions were shown to be the cause of local degradation of the resin by occurrence of water electrolysis. In spite of its significance, non-uniformity of the current distributions caused by the local changes in bed conductivity was not taken into account in the present investigation.

For resins saturated with copper ions, the current became higher as H^+ ions replace Cu^{2+} ions because of the higher conductivity of the H^+-form resin. This phenomenon is particularly visible for the softer resin saturated with copper ions, and fourfold increases in the current were recorded. For initial values of $\overline{X}_{Cu^{2+}}$ near 0.7, the current was found to increase with the 50WX-2 resin, and to decrease with the stiffer resin. Moreover, with resins poorly loaded with copper ($\overline{X}_{Cu^{2+}}$ below 0.5), fairly high currents were recorded at the beginning of the run, due to the significant presence of H^+ in the resin. The current decreased throughout the experiments with both types of resin, in spite of the progressive replacement of Cu^{2+} in the resin bed.

Applying Relations 9 and 10, shows that the potential gradient is not constant throughout the experiment. ΔE_{bed} and $\nabla\Phi$ were calculated at the arbitrary basis of the cell current averaged over the first hour: this is of restricted consequence since the potential gradient varied by less than 15% during the run, even with fully loaded resins.

4.4. *Copper in the cathode compartment*

The amount of copper ions transported from the ion-exchange bed to the cathode compartment, $n_{Cu^{2+}}$, against time is shown in Figure 6. In all cases, the amount of Cu^{2+} ions increased regularly with time, depending on the potential gradient over the bed, the initial fraction of copper in the resin, and the resin grade. Higher desorption and transfer rates were allowed by higher potential gradients, as expected. Higher rates were observed with the more flexible resin 50WX-2 and initial values for $\overline{X}_{Cu^{2+}}$ near unity. The final amount of Cu^{2+} ions recovered in the cathode compartment could exceed 3×10^{-3} mol with both resins, to be compared with the initial amounts sorbed of 6×10^{-3} and 13.5×10^{-3} mol for the 50WX-2 and HCR-S grades, respectively.

The number of moles of metal copper deposited on the cathode, $n_{Cu,m}$, was generally much lower than that of cupric ions. The amount of metal copper increased with the applied voltage, varying from 9.4×10^{-5} to 1.6×10^{-4} mol for ΔE_{bed} varying from 4.25 to 7.97 V with the 50WX-2 resin, and from 1.85×10^{-5} mol at 1.48 V to 8.51×10^{-5} mol at 10.08 V for the HCR-S resin. The initial concentration of Cu^{2+} in the resin was shown to also affect the amount of metal deposited even though no evident relationship between the two variables could be established.

Besides, the analysis of the liquid fractions collected from the anode side revealed the occurrence of side

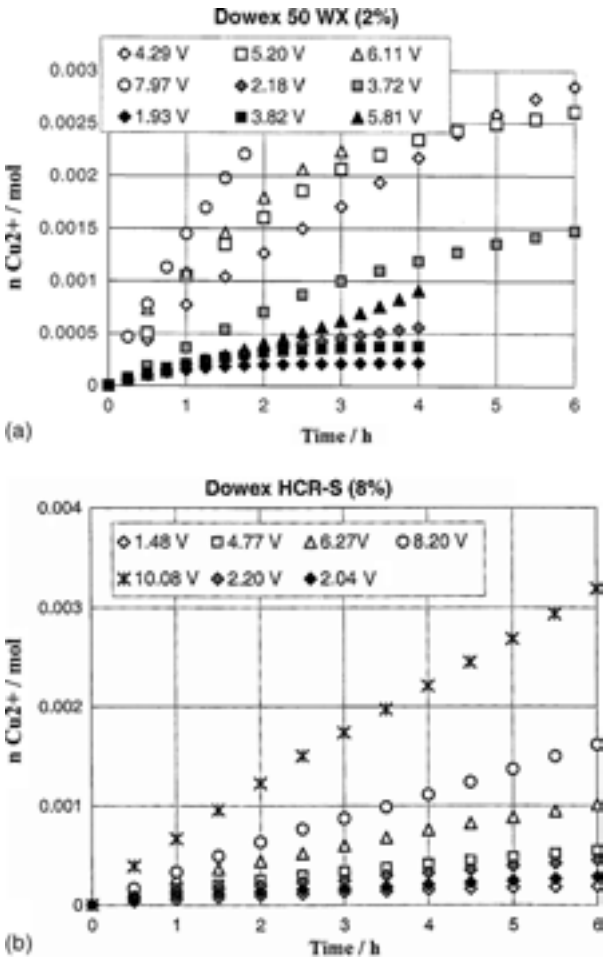

Fig. 6. Time variations of the number of moles of Cu^{2+} in the cathodic compartment for the two resins: (a) 50 WX-2; (b) HCR-S. Effect of potential difference in bed and initial impregnation of bed: white symbols refer to initial $\overline{X}_{Cu^{2+}}$ near 1, grey symbols are for intermediate value of $\overline{X}_{Cu^{2+}}$; dark symbols refer to the lowest initial value of $\overline{X}_{Cu^{2+}}$.

diffusion of Cu^{2+} ions to the anode compartment. The amount of Cu^{2+} ions accumulated in the anode compartment represents a few percent of that recovered in the cathodic solution. Finally, the concentration of copper ion in the liquid issuing from the packed bed is at ppm levels or below, and integration of the copper flux from the central compartment over time led to molar amounts below 10^{-5} mol in most cases. Mass balances on copper species were controlled for all experiments and were shown to hold within 15% in most cases.

For electromigration of nickel ions, Janssen et al. [8] proposed an empirical model of the resin regeneration, assuming first-order kinetics with respect to the metal ion concentration in the resin, and with a maximal amount of ions extracted from the resin, depending on the potential gradient. Neglecting the loss of Cu ions in the anode compartment and in the liquid issuing from the packed bed, the regular increase in Cu^{2+} ion concentration in the cathodic solution corresponds to the depletion of the resin. Therefore, applying the above model to the case of copper sulfate yields exponential laws for the number of moles of Cu^{2+} in the cathode compartment:

$$n_{Cu^{2+}} = n_{Cu^{2+},max} \times (1 - \exp(-t/\tau)) \tag{11}$$

where $n_{Cu^{2+},max}$ is the maximal quantity of copper ion in the cathode compartment at infinite time and τ is the time constant for the regeneration process. Experimental data were fitted to Equation 11.

4.5. *Current efficiency*

The ratio of the quantity of copper transferred to the cathode compartment and the charge passed during electrodialysis taking into account the faradaic constant, expresses the efficiency of copper transport induced by the electrical field. The integral current efficiency, $\Phi_{Cu^{2+}}$, is then expressed as

$$\Phi_{Cu^{2+}} = \frac{z_{Cu} F n_{Cu^{2+}}}{\int_0^t I\,dt} \tag{12}$$

Because a fraction of the copper cations transferred is reduced into metal copper, the current efficiency of the ion transfer can also be defined taking into account the copper deposited:

$$\Phi_{Cu} = \frac{z_{Cu} F [n_{Cu^{2+}} + n_{Cu,m}]}{\int_0^t I\,dt} \tag{13}$$

even though the two yields differ from each another by a few percentage points. The values of Φ_{Cu} are given in Table 2. For both resins saturated with copper, the current efficiency ranges from 25 to 45%. The efficiency is drastically reduced for partially impregnated resins as shown in Table 2: in such cases the current is essentially transported in the complex medium by highly mobile ions. The fraction of copper removed from the bed for a given electrical charge seems independent of the potential drop over the bed and the current efficiency is not affected by the cell voltage. This phenomenon is particularly observable for the 50 WX-2 resin.

In addition, the differential current efficiency between t_1 and t_2 can be defined as

Table 2. Values of the integral current yield of copper recovery in the cathode compartment after 4 h and of the apparent diffusion coefficient of copper ions in the packed bed inserted between the Nafion 117 membranes

Resin	$Y_{Cu^{2+}}$ initial	Current yield, Φ_{Cu}	$10^{11}\ D_{Cu,eff}$ /$m^2\ s^{-1}$
50 WX-2 (2%)	0.98	0.32–0.45	2.6–3.3
	0.61	0.13	2.4–2.7
	0.36	0.05–0.11	1.5–5.4
HCR-S (8%)	1.00	0.17–0.42	0.17–0.44
	0.73	0.10	0.34
	0.47	0.035	0.36

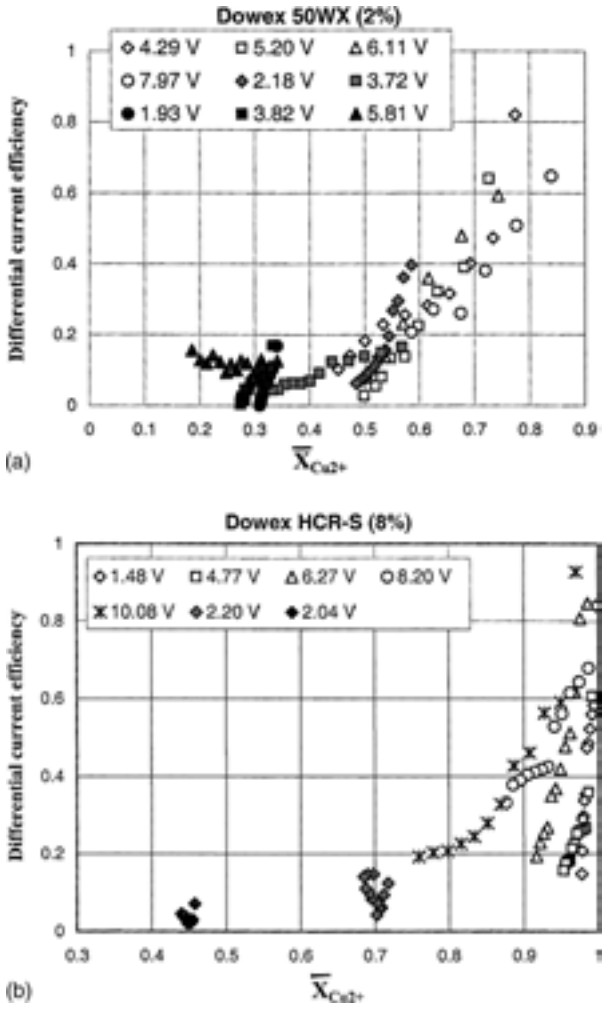

Fig. 7. Current efficiency of Cu^{2+} transfer to the cathodic compartment against molar fraction of copper ions in resin bed: (a) 50 WX-2; (b) HCR-S. Effect of potential difference in bed and initial impregnation of bed: white symbols refer to initial $\overline{X}_{Cu^{2+}}$ near 1, grey symbols are for intermediate value of $\overline{X}_{Cu^{2+}}$; dark symbols refer to lowest initial value of $\overline{X}_{Cu^{2+}}$.

$$\eta_{Cu^{2+}} = \frac{z_{Cu}F[n_{Cu^{2+}}(t_2) - n_{Cu^{2+}}(t_1)]}{\int_{t_1}^{t_2} I\,dt} \tag{14}$$

Figure 7 shows the relation between the differential current efficiency and the ionic fraction of Cu^{2+} remaining in the resin, as a function of cell voltage and initial concentration in the resin. The efficiency of Cu^{2+} transport reaches 100% at the first instants of electromigration runs when Cu-form resin predominates in the bed. The differential current efficiency for the regeneration process is strongly decreased by the presence of H^+ in the resin, even in the first hour, due to the side-transport of the current by the available protons. For all cases, the differential current efficiency was observed to decrease with time, due to the partial regeneration of the bed, most likely near the inlet of the cell. Since the diffusion coefficient of H^+ in the resin is an order of magnitude greater than that of Cu^{2+}, H^+ transport predominates, which reduces the regeneration rate and the differential current efficiency.

For the 50WX-2 resin, the differential yield is weakly dependent on the potential gradient and the initial amount of copper ions adsorbed on the resin (Figure 7(a)). For the more rigid resin, the rate of decrease does not only depend on the regeneration extent equal to $(1 - \overline{X}_{Cu^{2+}})$, and the plot does not suffice to explain the global behaviour of the process. For low potential gradient, $\eta_{Cu^{2+}}$ is shown in Figure 7(b) to decrease rapidly below 0.2 for low regeneration extents. This could be explained by observations of the bed during the runs: for such conditions, a small fraction of the bed at the bottom can be converted into H^+-form resin, and the current flows near exclusively through the regenerated part.

4.6. *Apparent diffusion coefficient of copper species*

Derivating Relation 11 and introducing A_{bed}, the cross-section of the packed bed for the current, leads to the expression of the specific flux, N_{Cu}:

$$N_{Cu} = \frac{n_{Cu^{2+},max}}{\tau A_{bed}} \exp\left(-\frac{t}{\tau}\right) \tag{15}$$

Equating 7 and 15, taking into account Relation 8 yields:

$$\frac{n_{Cu^{2+},max}}{\tau A_{bed}} \times \exp\left(-\frac{t}{\tau}\right) = \frac{z_{Cu}FD_{Cu,eff}[\overline{Cu}^{2+}]}{RT} \times \nabla\Phi \tag{16}$$

The ion concentration in the resin is involved in the above relation since the resin bed is much more conducting than the percolating liquid. Because the concentration of copper ions in the resin is assumed to decrease with time at the same rate than the specific flux, as discussed above, the apparent coefficient is simply deduced:

$$D_{Cu,eff} = \frac{n_{Cu^{2+},max}}{\tau A_{bed}} \times \frac{RT}{z_{Cu}F[\overline{Cu}^{2+}]_0 \nabla\Phi} \tag{17}$$

where subscript 0 refers to $t = 0$. It can be noticed that from the model assumptions, the apparent diffusion coefficient is constant throughout the regeneration of the resin bed, regardless of the form of the ion-exchange resin. The model developed here does not yield a rigorous description of the complex process. However, it is perfectly supported by the exponential profiles of the variations of $n_{Cu^{2+}}$ with time.

The values of this overall coefficient are reported in Table 2. For the 50WX-2 resin, the average apparent diffusion coefficient was found at $(3.0 \pm 0.4) \times 10^{-11}$ m^2 s^{-1}. For the HCR-S grade, the average apparent diffusion coefficient was equal to $(0.32 \pm 0.04) \times 10^{-11}$ m^2 s^{-1}. The average apparent diffusion coefficient in 50 WX-2 and HCR-S resins, represents 1/25 and 1/

225, respectively, of the corresponding coefficient in the water. In addition, these coefficients are roughly three times lower than the predicted diffusion coefficient in a resin particle (Section 3). The deviation has the following reasons: first, the apparent diffusion coefficient yields an overall description of diffusion/migration phenomena in the packed-bed, and not in isolated particles, as for $\overline{D}_{Cu}$: the two diffusivities have different physical meanings. Besides, the presence of the membrane is to result in additional hindrance to ion transfer, and this point should be confirmed by further investigations.

5. Conclusion

Elementary processes involved in the operation of hybrid ion-exchange electromigration process have been investigated for the case of copper sulfate solutions. First the adsorption equilibrium of cupric ions has been determined depending on the solution pH and the cross-linking degree of the Dowex resins. Secondly, the electromigration of cupric ions in the resin bed under an applied electrical field has been thoroughly observed with formerly impregnated beds: the current efficiency of the desired migration can attain 100% for fully impregnated resins and the rates are governed by the potential gradient and the stiffness of the resin. The transport rates and the current efficiency are drastically reduced for partially impregnated resins since the current flow is strongly favoured by the presence of highly mobile ions in the solid phase. Non-uniform composition of the bed alters dramatically the yields and the regeneration of Cu-form regions can hardly be achieved due to the above short-circuit phenomena.

A more suitable design of the three-compartment cell has to searched for higher performance, with a view to larger applications of the hybrid process for the treatment of dilute solutions.

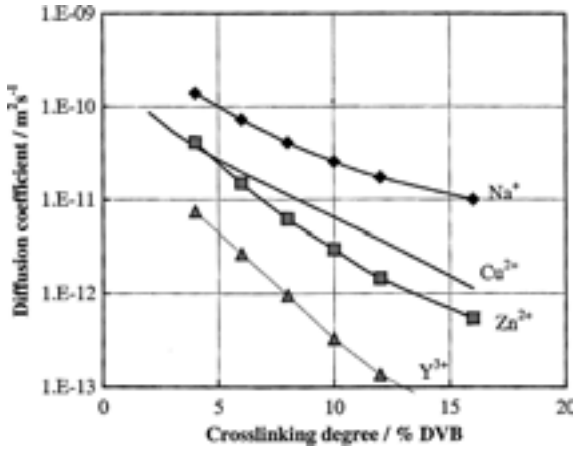

Fig. 8. Diffusion coefficient of metal ions in ion-exchange resins depending on the cross-linking degree: comparison of the values for Cu^{2+} ion calculated from [20] with experimental data obtained by Boyed and Soldano [21].

Acknowledgements

The costs of the exchange of scientists (S.V. and A.A) were covered by NATO within the Science for Peace Program (contract 972490). Thanks are also due to Patrick Carré for technical assistance in the construction and development of the experimental set-up.

References

1. K. Jüttner, U. Galla and H. Schmieder, *Electrochim. Acta* **45** (2000) 2575.
2. L.J.J. Janssen and L. Koene, *Chem. Eng. J.* **85** (2002) 137.
3. E. Glueckauf, *Brit. Chem. Eng.* **4** (1959) 646.
4. G.C. Ganzi, Y. Egozy and A. Guiffrada, *Ultrapure Water* **4** (1987) 43.
5. G.C. Ganzi, A.D. Jha and J.H. Wood, *Ultrapure Water* **14** (1997) 64.
6. R. Flucht, L. Furst, H. Neumeister and R. Nguyen, *Ultrapure Water* **13** (1996) 60.
7. J.A. Wesselingh, P. Vonk and G. Kraaijeveld, *Chem. Eng. J.* **57** (1995) 75.
8. P.B. Spoor, W.R. ter Veen and L.J.J. Janssen, *J. Appl. Electrochem.* **31** (2001) 523.
9. P.B. Spoor, W.R. ter Veen and L.J.J. Janssen, *J. Appl. Electrochem.* **31** (2001) 1071.
10. F. Helfferich, 'Ion Exchange' (McGraw-Hill, New York, 1962).
11. K.H. Lin, *AIChE Symposium Series*, No. 152, **71** (1975) p. 86.
12. J. Semmens, *AIChE Symposium Series*, No. 152, **71** (1975) p. 214.
13. T. Kodama and S. Komarnemi, *Sep. Sci. Technol.* **34** (1999) 2275.
14. I. Zouari and F. Lapicque, *Electrochim. Acta* **37** (1991) 439.
15. S. Wasyljiewicz, *Fluid Phase Equilibria* **57** (1990) 277.
16. R.H. Perry and D.W. Green, 'Perry's Chemical Engineers' Handbook', 7th edn (McGraw-Hill, New York, 1997).
17. F. Dardel, 'Echange d'ions', Techniques de l'Ingénieur J2783 (Paris, 1998).
18. H.M. Verbeek, L. Fuerst and H. Neumeister, *Comp. Chem. Eng.* **22** (1998) S913–S916.
19. P.N. Dwidedi and S.N. Upadhay, *I.E.C. Process Design Dev.* **16**(2) (1977) 157.
20. T. Kataoka, H. Yoshida and H. Sanada, *J. Chem. Eng. Japan* **7** (1974) 105.
21. G.E. Boyed and B.A. Soldano, *J. Am. Chem. Soc.* **75** (1953) 6091.

Appendix

The film thickness was calculated using the relation proposed by Dwidedi [19] for the external mass transfer rate:

$$k_d = 1.1 \times \frac{v}{\varepsilon} \frac{Re_p^{-0.72}}{Sc^{2/3}} \qquad \text{for } Re_p < 10 \tag{18}$$

as it was established by compilation of various sources of data. Re_p is the particle Reynolds number, defined on the average diameter of the resins and v, the superficial velocity of the solution, and ε the bed porosity. The parameters selected for the calculation

were: $v = 0.425$ mm s^{-1} (corresponding to 2 ml min^{-1} in the column), $\varepsilon = 0.40$, $v = 10^{-6}$ m^2 s^{-1}, $D_{Cu} = 7.2 \times 10^{-10}$ m^2 s^{-1}. The average particle radius was taken as 112 and 285 μm for resins 50WX-2 and HCR-S, respectively. The thickness of the diffusion film defined as the ratio (D_{Cu}/k_d) was found at 14.2 and 27.7 μm for the two resins used.

The diffusion coefficient of copper ion in the resin was estimated using the empirical correlation proposed in [20], as follows:

$$\frac{\overline{D}_{Cu}}{D_{Cu}} = 0.55 \times \exp\left[-0.174 z X_{cl}\left(\frac{V_H^w}{V}\right)\right] \tag{19}$$

where z is the valence of the copper ion, V_H^w is the volume of H-type resin in the water and V, the volume of all forms of resin in the solution. The ratio of the two volumes appearing in Relation 19 can be calculated [20]:

$$\frac{V_H^w}{V} = [1 - 0.52(z[Cu^{2+}] - 1)\exp(-0.205X_{cl})] \times \exp\left[0.023\frac{M_{Cu}}{z}(1.51 - 0.51z[Cu^{2+}])\exp(-0.192X_{cl})\right] \tag{20}$$

where M_{Cu} is the molecular weight of Cu^{2+} ions. The calculations were carried out for a concentration of cupric ions of 0.25 M varying X_{cl} (%) from 2 to 16, even though the original law was established for X_{cl} greater or equal to 3, and considering the value of D_{Cu} at infinite dilution and at 25 °C (i.e., 7.2×10^{-10} m^2 s^{-1}). As expected, the estimated diffusion coefficient decreases with the crosslinking degree, varying from 8.7×10^{-11} to 1.1×10^{-12} m^2 s^{-1} when X_{cl} (%) passes from 2 to 16 (Figure 8). The predicted variation is in satisfactory agreement with the experimental values of the diffusivity of other ions obtained by Boyed and Soldano [21] and reported in [10]; in particular, the data for Cu^{2+} ion are fairly close to the experimental data for Zn^{2+} ion (Figure 8).